EXECUTIVE SUMMARY OF THE THESIS

Injectable gelatin-based photocurable composite hydrogel for the treatment of osteochondral defects

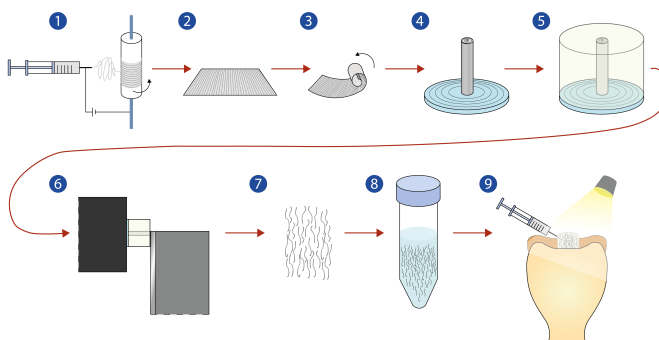LAUREA MAGISTRALE IN BIOMEDICAL ENGINEERING - INGEGNERIA BIOMEDICA

Author: IGNAZIO NIOSI

Main Advisor: Prof. Silvia Farè

External Advisor: Prof. Leonardo Ricotti

Co-advisors: Lorenzo Vannozzi, Diego Trucco

Academic year: 2021-2022

Graphical abstract

Figure 1: Steps involved: (1) Rotating set-up for aligned fibers mesh. (2) Electrospun mesh. (3) Preparation of the mesh for micro-cutting technique. (4) Sample positioning. (5) Embedding of the sample in cryomedium. (6) Cryomicro-cutting technique. (7) Dispersed fibers (DFs). (8) Filling step on hydrogel solution. (9) Injection and UV-curing step.

1. Introduction

Chondral and osteochondral defects (OD) are lesions that occur as consequent of deseases, like osteoartrithis, and traumatic events, leading towards an irreversible ongoing degenerative process. Injuries of this type affect people of all ages and are more frequent in bearing joints. The regenerative capacity of this tissue is very poor, and for diseases where the OC defects are either cause or effect of the ill condition, the pathophysiological mechanisms govern the processes are still not fully known. Among possible available therapies, regenerative approaches have as their main limitations the open surgery and related problems such as increased risk of infection and hospitalisation, the matching site implantation with related iatrogenic conditions and for some of them the high costs related to cell use and manipulation. Additionally, none of the presented limitations is supported by excellent clinical outcomes for the corresponding regenerative approach. For this reason, research is shifting towards the development of minimally invasive injectable devices that might overcome or partially reduce the ef-

fects caused by the regenerative treatments, at least guaranteeing the same clinical outcomes. Among possible materials, hydrogels represent a class of biomaterials that lend themselves to this type of use, due to their excellent cell-friendly properties, their high aqueous content that mimics the extracellular matrix and the possibility of being injectable materials enjoying shear thinning behaviour. Gelatin materials, in particular gelatin methacrylate (GelMA), have seen widespread use for OC applications due to the possibility of modulating their chemical-physical properties, in combination with the use of fabrication techniques as 3D printing, acted to obtain mechanically performing structured systems, suitable for bearing tissue substitutes. However, conceiving GelMA as an injectable system, involves having the main limitation of poor mechanical properties. For this reason, both the possibility of inserting synthetic components (i.e., as semi- or interpenetrated polymer networks, or copolymer systems) and fillers has been investigated. Among the possible fillers to be used to increase mechanical properties, fiber-based fillers have attracted particular interest. The possibility to obtain dispersed fibers (DFs) [1] [2] using fibers mesh made of biopolymers, like poly-ϵ-caprolactone (PCL) or poly(lactic-co-glycolic) acid (PLGA), through post-processing techniques as ultrasonication and micro-cutting techniques, has been investigated. In light of this, the overall objective of this work is to investigate and develop an interpenetrated IPN injectable system, consisting of a network of GelMA and polyvinyl acohol (PVA), with a PCL:GelMA dispersed fiber-based filler, with enhanced compressive mechanical performance. In this thesis work, the rheological and injectability properties of GelMA were investigated, followed by the fabrication and post-processing of an electrospun mesh to obtain DFs, in addition to a post-crosslinking compressive mechanical characterization on the GelMA+DFs assembly. Better mechanical properties of the composite were demonstrated compared to the GelMA network alone. An ideal range of temperature and injection parameters were identified in order to be able to inject in comfortable force ranges, according to EN ISO 7886 1:2018.

2. Materials and Methods

The thesis workflow was as follows: synthesis, rheological characterization and injectability of GelMA. Fabrication and post-processing of electrospun meshes in order to obtain DFs. Morphology evaluation on DFs and on both bulk composite and GelMA crosslinked hydrogels. Mechanical compression evaluation of composite GelMA+DFs.

2.1. GelMA synthesis

Gel was soaked in pre-heated 50 °C PBS at 10 % w/v concentration and 0.6 g for each gram of Gel was added and left to react for 2 h. The obtained solution was then purified and freeze dried to obtain GelMA flakes with a degree of functionalization of $\approx$ 80 %.

2.2. Electrospun mesh and DFs fabrication

A PCL75:GelMA25 (ratio 3:1) at 20 % w/v concentration in AA was prepared to fabricate aligned electrospun mesh with a hommade set-up (Fig.2). The electrospun parameters setted were: 2000 rpm/min rotating mandrel, 16kV applied electric field, 0.5 ml/h flow rate, 13 cm distance between sirynge and collector and 1 h of electrospinning time process. The obtained mesh was opportunely cutted (1x1 cm), rolled to form a cylindric sample and then micro-cutted with a cryostat (YD-1900, JINHUAYIDI) with a thickness cut of 20 μm), as reported in Fig.3.
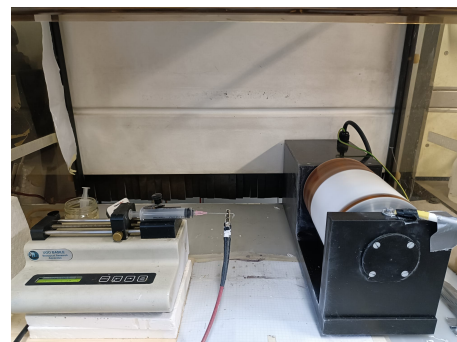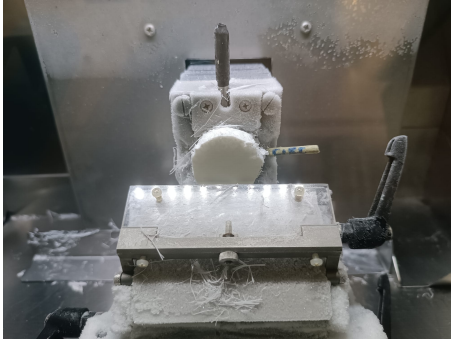

Figure 2: Hommade set-up: rotatic mandrel.

Figure 3: Cryostat microcutting configuration.

2.3.   Rheological analysis

An Anton Paar modular compact rheometer (MCR 302e) equipped with a 50 mm diameter cone-plate configuration was used for the rheological analysis on 10% GelMA solution in DIW. Flow analysis, amplitude and ramp decreasing temperature sweep and viscosity vs temperature tests were conducted. For flow analysis and amplitude sweep the the tests were performed at 20, 25, 30 and 37 ° C.

2.4.   Injectability

Injectability tests on 10% w/v GelMA in DIW solution were performed by using homemade developed set-up adapted to a MTS electromechanical machine (MTS, cat no. 1/MH with CTD-200, thermal chamber) with a thermostatically controlled chamber using a 5 kN load cell. The test was carried out at four operating temperatures (20, 25, 30 and 37 °C) with a 5mL syringe and for 18G, 20G, 22G needle types. The crossbeam velocity was set at 1.63 mm/sec corresponding to a 0,2 mL/sec folw rate.

2.5.   Photo-crosslinking step

GelMa was dissolved in DIW at a concentration of 10 % w/v. To obtain the DFs-loaded GelMA (GelMA+DFs), the DFs at 0.5% w/v were added separately to the GelMa solution. Separately a solution of Irgacure 2959 with a 0.5% w/v concentration was prepared in DIW at 80° C. Then, the GelMA and cooled Irgacure solutions were mixed in order to have a photo-crosslinking upon exposure to UV light. A cylindrical mold (diameter: 7 mm, height: 5 mm) was used to poured both solution to perform the photo-crosslinking at 365 nm (Lightniningcure LC5 lamp, Hamamatsu) with a UV light intensity of 3,5 W/cm^2 for 2 min'.

2.6.   Morphological analysis

Both electrospun mesh, DFs and lyophylized UV-crosslinked samples (GelMA and GelMA+DFs) were scanned (Phenom XL, Thermo Fisher Scientific) to evaluate the resulting dimension of the fibers and directionality, the shape and morphology of DFs, and the porosity, pores dimension and DFs bulk integration respectively.

2.7.   Mechanical compression tests

An Instron 5965 machine equipped with 1kN load-cell was used to carry out the mechanical tests on photo-crosslinked samples. A compression deformation rate of 1 mm/min was applied. The photocrosslinked GelMA and GelMA+DFs samples were immediately subjected to compression at room temperature. The compressive modulus from the linear region of the curves, calculated as the slope of the curve in the range 0-10%. Compressive toughness, maximal deformation and strength were additionally calculated for compression mechanical cheracterization.

3.   Results and Discussion

3.1.   Rheological analysis

Flow analys showed the shear-thinning behaviour of the GelMA solution at different temperature with a more sensitivity near the sol-gel temperature, suggesting the consistency of flow of the material (Fig.4a. Amplitude sweep test performed at different temperatures ensured the identifincation of a common linear viscoelastic region, giving us information about a solid rather than liquid-like behaviour associated to the material. At 30 and 37 ° C the material showed a more liquid-like behaviour with fluctuating value of G' and G" for 0.1-1 % strain. Going towards cooler temperature a more solid-like behaviour is associated to the material and the G' and G" did not change for all range of strain. Decreasing ramp temperature sweep and viscosity vs temperature respectively reported in (Fig.4b. Figs.4c and 4d, confirmed the location of sol-gel temperature near of 20° C, suggesting the possibility of the material to be injectable in its surroundings.
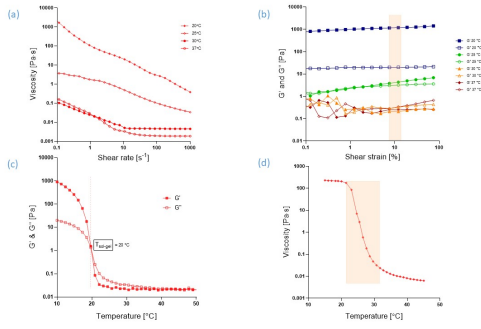
Figure 4: Representative curves: (a) Viscosity vs shear rate. (b) Amplitude sweep. (c) Decreasing ramp temperature sweep. (d) Viscosity vs temperature.

3.2. Injectability

The injection force decreased with increasing temperature, as suggested from the viscosity vs temperature rheological investigation. At 20 ° C the material was not able to be extruded. It posses a gelly brittle behaviour with an increasing trend in force (test was manually interrupted to avoid collapse of set-up). At 25 ° C the extrusion proceeded, showing a pseudo-plateau region, maybe due to a partial gelation of some spots within the material. For 30 and 37 ° C the injection occurred showing smoother profiles and relative low force (< 10 N) for all needle tested. In Fig. 5 is possible to observe what was described. A limit temperature value for effective comfortable injection was set at 30 ° C, especially for both 18G and 20G needles.
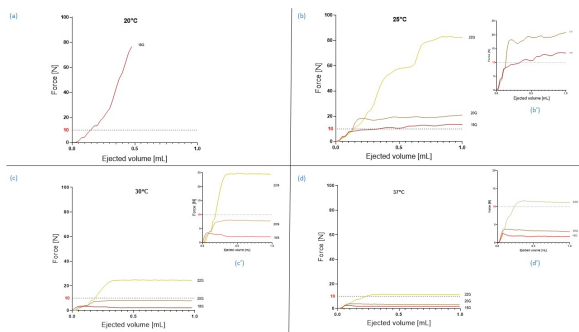

Figure 5: Representative force-extruded volume curves: (a) At 20 ° C, brittle gel exstrusion. (b) At 25 ° C no reaching of a well defined plateau-region. (b') Rescaled graph. (c) At 30 ° C smooth profile curves. (c') Rescaled graph. (d) At 37 ° C lowest required forces. (d') Rescaled graph.

3.3. Morphological analysis

The aligned electrospun meshes displayed no beads in their surface and a high desired direc-

tionality (Figs.6a and 6b. After the cryomicro-cutting technique were obtained two main microstructured elements: DFs (Fig.7a) and strip-like structures (Fig. 7b). A measured characteristic dimension of ≈ 20 μm was associated with both filler types. For DFs it was hypothesised that, supported by Fig.8a and 8b, a reinforcing mechanism was established by the interaction between the DFs and the GelMA network. These were likely to adhere and bind chemically well in the GelMA network because even after freeze-drying they assumed the shape as in the Figs.8, without suffering a collapse. This appearance might be attributed to the GelMA component in the DFs.

In order to narrow the characteristic dimensions of the obtained microstructured elements, a possible implementation of different set-up for aligned fibers fabrication should be designed.
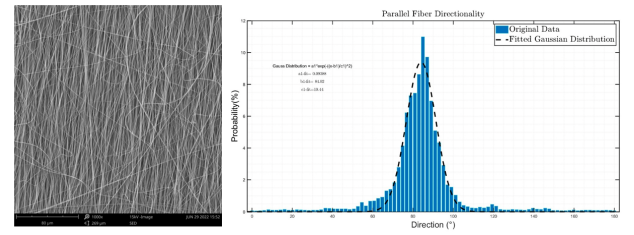

Figure 6: Aligned mesh: (a) No-beads morphology, 1000x, scale bar= 80 μm. (b) Directionality histogram, narrow and sharp at around 90° .

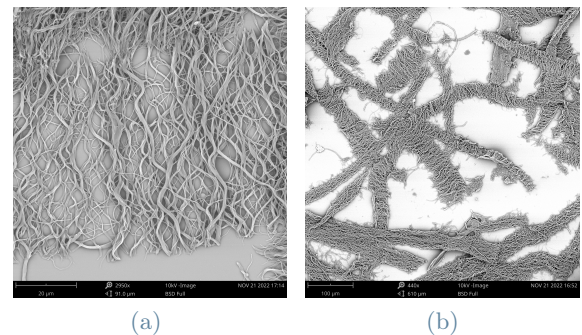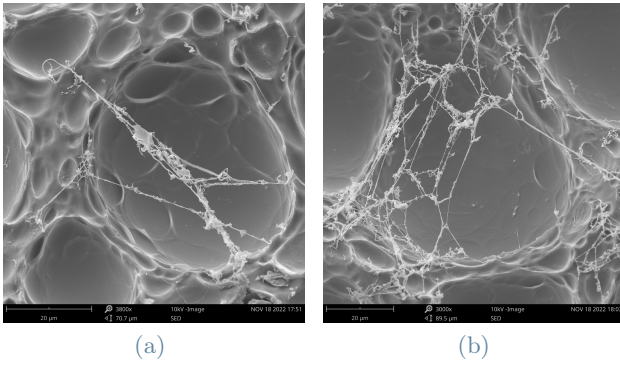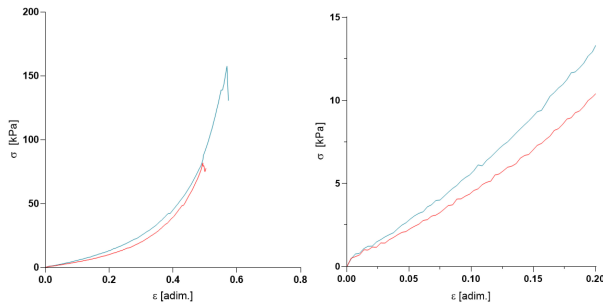(a)   (b)

Figure 7: (a) DFs, 3500x, scale bar= 20 μm. (b) Strip-like microstructures, 440x, scale bar= 100 μm.

.

(a)   (b)

Figure 8: Representative examples of intertwined DFs adhering in different points of bulk network material. (a) 3800x, scale bar= 20 μm. (b) 3000x, scale bar= 20 μm.

3.4. Mechanical compression tests

Figure 9: Stress-strain: Representative curve (left). Magnification of the linear region for 0-20% deformation (right).

Composite reached high maximal strength values, that correspond to the once at brake, of up to 150 kPa, increasing the value by 100% compared to the GelMA alone. Maximal deformation exhibited an increasing of its value up to $\approx 60\%$. The area subtended by the stress-strain curve was consequently larger, which might be associated with a greater toughness for composite material. GelMA+DFs exhibited a stiffer behaviour and did not acquire a fragile one. New character to the stress-strain curve was observable in Fig.9, where a higher slope was associated to the GelMA+DFs curve.

The calculated values of compressive modulus, maximal deformation, maximal strength and compressive toughness for GelMA+DFs were 70.8 ± 5.8, 60.8 ± 2.6, 139.3 ± 10 and 4 ± 0.19 respectively.

(a)   (b)

(c)   (d)
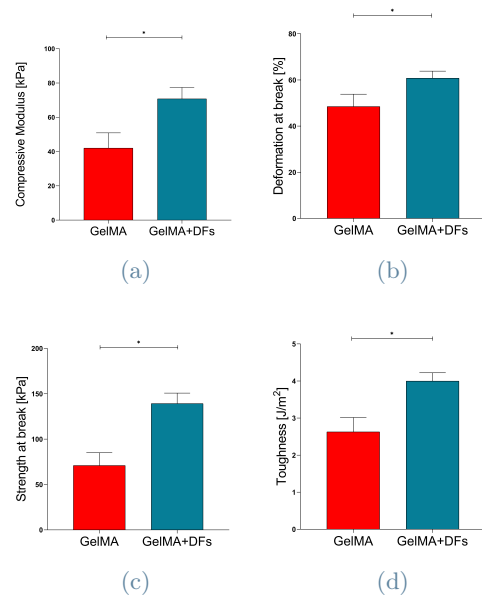
Figure 10: GelMA (red) and GelMA+DFs (light blue): (a) Compressive Modulus. (b) Maximal deformation. (c) Maximal strength. (d) Compressive toughness. (*p-value < 0.05).

The DFs acted therefore in the GelMA network as reinforcing fillers. This characteristic might be related both to the intrinsic nature of the PCL component in the DFs, but also due to the 3D distributoin of the DFs in the bulk, which might bear part of the load, thus guaranteeing a strengthening of the composite. Additionally it was likely that the DFs increased stiffness for low deformation values by acting as rigid elements, while deformed greatly for gradually increasing deformations, once embedded in GelMA+DFs to form the composite.

4. Conclusions and future developments

In this study, it shown that through a cryomicrocutting technique post-processing on optimized electruspun meshes of aligned fibers, was possible to obtain mono DFs and organized strip-like microstructures composed of fibers.

Moreover, the mechanical compression performance for the composite GelMA+DFs increased as expected almost doubling respect to GelMA network alone due the the DFs presence.

A range of temperature for a feasible GelMA injection attested between 30 and 37 ° C for all the needles tested (18G, 20G, 22G), according

to EN ISO 7886 1:2018. The reaching of the a plateau force region indicated a homogeneous extrusion of materials. A value of force of $\approx$ 10 N settled a limit value for consider an injection process comfortable suggesting that 22G is an unsuitable needle. Near the sol-gel transition temperature, the material was uninjectable assuming force injection profile that never reached a plateau.

Some experimental tests are still ongoing, e.g., the injectability force, the swelling behavior and the sol fraction featuring the GelMA + DFs material. These results would complete the set of experiments concerning this thesis.

Therefore, the study reported a novel composite consisting of microstructured fiber elements dispersed in a GelMA network, with enhanced mechanical properties, that might be capable of be used as mini-invasive system for osteochondral application.

However, for a better dispersion of DFs, the implementation of a new set-up for the fabrication of electrospun analigned meshes with a single filament configuration should be an option to obtain fibrous microelements in a narrower size range.

Additionally, the implementation of a synthetic component to design an IPN structured, will be investigated coupled with a wider injectability configurations also for GelMA+DFs composite, in order to increase the baseline of bulk material mechanical properties, aiming to reach value of tenths of MPa for compressive modulus to have stiff comparable properties with the one of natural articular cartilage [3].

Cells adhesion tests, viability and cytotoxicity assays, in addition to chondro and osteogenic potential will be carried out to asses the GelMA+DFs composite applicability in possible future trials.

5.   Acknowledgements

References

[1] Paria Ghaderinejad, Najmeh Najmoddin, Zohreh Bagher, Mahdi Saeed, Sarah Karimi, Sara Simorgh, and Mohamad Pezeshki-Modaress. An injectable anisotropic alginate hydrogel containing oriented fibers for nerve tissue engineering. *Chemical Engineering Journal*, 420:130465, 2021.

[2] Abdolrahman Omidinia-Anarkoli, Sarah Boesveld, Urandelger Tuvshindorj, Jonas C Rose, Tamás Haraszti, and Laura De Laporte. An injectable hybrid hydrogel with oriented short fibers induces unidirectional growth of functional nerve cells. *Small*, 13(36):1702207, 2017.

[3] Xiangbo Zhu, Taijun Chen, Bo Feng, Jie Weng, Ke Duan, Jianxin Wang, and Xiaobo Lu. Biomimetic bacterial cellulose-enhanced double-network hydrogel with excellent mechanical properties applied for the osteochondral defect repair. *ACS Biomaterials Science & Engineering*, 4(10):3534–3544, 2018.